Failure Diagnosis of a Gear Box by Recurrences

Arkadiusz Syta
Lecturer
Department of Applied Mathematics
Technical University of Lublin
PL-20-618 Lublin, Poland
Email: a.syta@pollub.pl

Józef Jonak
Professor
Department of Machine Construction
Technical University of Lublin
PL-20-618 Lublin, Poland
Email: j.jonak@pollub.pl

Łukasz Jedliński
Graduate Research Assistant
Department of Machine Construction
Technical University of Lublin
PL-20-618 Lublin, Poland
Email: l.jedlinski@pollub.pl

Grzegorz Litak*
Professor
Department of Applied Mechanics
Technical University of Lublin
PL-20-618 Lublin, Poland
Email: g.litak@pollub.pl
and
Department of Architecture, Buildings and Structures
Polytechnic University of Marche
Via Brecce Bianche
I-60131 Ancona, Italy

ABSTRACT

The recurrence analysis method is used in the mechanical diagnosis of a gear transmission system using time domain data. The recurrence is a natural behavior of a periodic motion system, which tells the state of the system, after running some time, will approach to a certain past state. In this paper, some statistical parameters of recurrence qualification analysis are extensively evaluated for the use of mechanical diagnosis, based on fairly short acceleration time series; recurrence results are compared with those obtained from Fourier analysis, and the identification procedures for the failure gear transmission by recurrences is also presented. It is found that, only using fairly short time series, some statistical parameters in quantification recurrence analysis can give clear-cut distinction between health- and damage-state.

*Address all correspondence for other issues to this author.

Nomenclature

$\mathbf{x}_i$,$\mathbf{x}_j$ Vector representation of the system states in discrete time i, j.
ε Threshold value.
RR, LAM, DET, L, TT
$VENTR$, $LENTR$ Parameters defined in the Recurrence Qualification Analysis.
$\bar{y}$ Average value of parameter y.
σ_y Standard deviation of parameter y.
$Kurt_y$ Kurtosis of parameter y.
$\mathbf{R}_{i,j}$ Recurrence matrix.
$P(l)$, $P(v)$ Histograms of the line diagonal and vertical lengths (l and v, respectively).
$p(l)$, $p(v)$ Normalized probability distributions of the line diagonal and vertical lengths (l and v, respectively).
PS Power spectrum.
$\Theta(x)$ Heaviside step function.
H1,H2 Signals corresponding to healthy gears measured by sensor No. 1 and 2, respectively.
D1,D2 Signals corresponding to damaged gears measured by sensor No. 1 and 2, respectively.
n Number which indicate the rotation interval.

1 Introduction

Gear transmission systems are widely used in real life because of their reliability and possibility of long time operation [1–5]. Due to backlash and time-varying mesh stiffness they show complex nonlinear response [6] such as chaotic vibrations [7]. Additionally, transmission errors can occur due to the wear phenomena and disturb the efficient work [8–10]. Operational safety requires to detect those defects before admitting the transmission system for a longer operation. The goal of the present note is to compare dynamics of the faulty transmission to the healthy one using nonlinear time series method of recurrence plots. For testing purposes, we used a single-stage transmission gears pair with angular teeth mounted on an industrial test stand [11]. This kind of gears is widely used in aircraft industry, e.g. to transmit power into the tail rotor in helicopters.

In the present paper, instead of using a standard frequency analysis [12], we calculate recurrence indicators from fairly short experimental time series of acceleration measured in different stages of the dynamical experiment. Finally, recurrence indicators are used to assess the gear usability and/or degradation. We assume that the faults occurred in the system introduce strongly nonlinear phenomena like friction and/or backlash that can influence the stability of the whole system. To search and identify such disturbing effects in the system dynamical response, we used a recurrence quantification analysis (RQA) which gives reliable indicators for system technical conditions [13–15].

2 Recurrence quantification analysis

Recurrence is a natural behaviour of the periodic motion when after some time the actual state of the system is close to a certain past state. Let $\mathbf{x}_i$ denote a state of a dynamical system at discrete time. Similarly, let $\mathbf{x}_j$ denote a different state of the examined system. Consequently, a recurrence phenomenon implies those states to be close to each other (after some time), what can be written as:

$$|\mathbf{x}_i - \mathbf{x}_j| \leq \varepsilon, \quad \text{for} \quad i \neq j. \tag{1}$$

This fact can be described in logical values (0 or 1) using the recurrence matrix:

$$R_{i,j}(\varepsilon) = \Theta(\varepsilon - ||\mathbf{x}_i - \mathbf{x}_j||), \quad \text{for} \quad i, j = 1, .., n, \tag{2}$$

where $||.||$ is the Euclidean measure, and $\Theta(x)$ is the Heaviside step function.

The results of the recurrence function (Eq. 2) that acts on the trajectory of the length n can be represented as a $n \times n$ matrix made of zeros and ones where rows and columns are marked as a discrete time. Its graphical representation of that matrix (coloured points (i, j) for $R_{i,j}(\varepsilon) = 1$, and empty places (i, j) for $R_{i,j}(\varepsilon) = 0$) is called a Recurrence Plot (RP) [16, 17]. Note that every recurrence plot includes a single point. More recurrences can be reflected into RP as vertical, horizontal lines or singular points. The points in RP can also form some other patterns possessing elements of vertical, horizontal lines. Thus, one can distinguish different kinds of motion just from recurrence plot topology.

However, a more specific investigation based on the statistics of points and lines forming the plot can be made (RQA - Recurrence Quantification Analysis) [17–20]. The RQA includes a few measures based on horizontal and vertical line patterns in terms of the statistical properties of line lengths and their distributions. Note, the diagonal lines represent the

periodic motion, while the isolated point reports a single recurrence that could appear by incidental passing through the same state in the phase space.

Recurrence rate RR:

$$RR = \frac{1}{n^2} \sum_{i,j=1}^{n} R_{i,j}(\varepsilon), \tag{3}$$

is the ratio of the recurrence points to all possible points.

Determinism DET:

$$DET = \frac{\sum_{l=l_{min}}^{n} lP(l)}{\sum_{l=1}^{n} lP(l)} \tag{4}$$

shows the contribution of points forming diagonal lines. $P(l)$ is a histogram of diagonal lines of length l.

Laminarity LAM:

$$LAM = \frac{\sum_{v=v_{min}}^{n} vP(v)}{\sum_{v=1}^{n} vP(v)} \tag{5}$$

shows the contribution of points forming vertical lines. $P(v)$ is a histogram of vertical lines of length v. DET and LAM show how many recurrence points are included in various diagonal and vertical lines. The first one (DET) used to characterize how periodic is the system dynamical response while the second (LAM) identifies small (laminar) changes in recurrences by calculating the ratio of small deviations in the recurrences to all recurence points. Interestingly, small deviations in recurrences are represented by vertical lines in RP.

The average length of diagonal lines L:

$$L = \frac{\sum_{l=l_{min}}^{n} lP(l)}{\sum_{l=l_{min}}^{n} P(l)} \tag{6}$$

can reflect the time correlation of time series, which is related to the average time of a periodic motion.

The average length of vertical lines called trapping time TT:

$$TT = \frac{\sum_{v=v_{min}}^{n} vP(v)}{\sum_{v=v_{min}}^{n} P(v)} \tag{7}$$

is a similar indicator to L but defined for vertical lines, which can tell about the characteristic time of a laminar motion. The Shannon entropy for diagonal lines L_{entr}:

$$LENTR = -\sum_{l=l_{min}}^{n} p(l) \ln p(l), \tag{8}$$

where $p(l)$ is probability of finding a diagonal line of length l.

The Shannon entropy for vertical lines V_{entr}:

$$VENTR = -\sum_{v=v_{min}}^{n} p(v) \ln p(v), \tag{9}$$

where $p(v)$ is probability of finding a vertical line of length v. Note, the parameters $LENTR$ and $VENT$ are particularly sensitive to noise.

The maximum length of diagonal and vertical lines is $LMAX$ and $VMAX$, respectively.

These quantities, or more precisely changes of their values in the system conditions, illustrate the dynamics of the underlying system. E.g. DET in a periodic system (long diagonal lines and few single points) takes a higher value than in a stochastic system (only single points). Note that the correct results of the RQA depend on proper choice of the embedding parameters (embedding dimension and embedding time delay). Furthermore, a subspace of all measured coordinates can be used.

3 The experimental set-up and results

We have tested single-stage transmission gears with angular teeth. The scheme of the gears and the location of the acceleration sensors are shown in Fig. 1.

The gears were dismounted and examined carefully after being in operation for a long time. It appeared that the gear system had been damaged, therefore the transmission system was replaced by a new (healthy) one and run again. We have recorded the vibration of acceleration in three directions (x,y,z) with a sampling frequency of 40 kHz for both damaged and healthy systems.

The damage of the transmission occurred after 3 hours and 15 minutes of the gear system work. The stop signal was due to the presence of a chips sensor. There has been a blurring effect due to the incorrect assembly of gears. The acceleration data was recorded regularly since the beginning of transmission to the occurrence of the damage.

More detailed analysis of the dismounted gears provided evidence that the lateral surface of the teeth had been damaged. The transmission system was replaced by the new (healthy) one and run again. The pinion had 19 teeth and was rotating with speed of 6196 rpm, and the driven wheel had 42 teeth. The data consists of 160 revolutions of the pinion, which correspond to 61960 points of the system evolution and a run time of 1.549 seconds. For the purpose of our analysis we divided the whole period into 10 rotation intervals, each of 16 revolutions.

In this project we compare the system response records obtained from two piezoelectric triaxial sensors. To obtain more information, than from the Fourier analysis, we apply the method of recurrence plots. Initial results related to this gear system have been recently reported by Jedliński at al. [11] who used frequency domain analysis. He filtered the measured signal to find differences between the healthy and faulty transmission gears. In the present approach, instead of using a filtering algorithm, we propose to use the simultaneously recorded data from 3 directions. The obtained data form vectors of the phase space.

Thus, we focus on comparison of the two different time series for faulty and healthy gears, recorded with a single 3d sensor (No. 1 in Fig. 1). As expected, the sensor No. 2 (Fig. 1) gave similar results (see Tab. 1). The corresponding time series for the healthy and damaged gears are presented in Fig. 2. Note that the wider distribution of measured points is clearly visible for the faulty gear pair (Fig. 2b). In Tab. 1 one can compare Basic statistical parameters including mean values, standard deviation and kurtosis used for all 3 directions, i.e. x, y, and z are compared in Tab. 1.

Comparing the statistics obtained, higher mean values for acceleration of healthy gears in y and z direction (H1) can be noted. On the other hand, the standard deviation of acceleration in the same direction is higher for the signal D1 of the damaged gears. The time series obtained from the second sensor behave in a similar way (almost all statistic parameters take higher values for signal D2). Interestingly, kurtosis is clearly larger for the damaged systems (Kurt $\gtrsim 3$, $i = x,y,z$) as compared to the healthy ones (Kurt$_i \lesssim 3$ where $i = x,y,z$). All estimated kurtosis values are relatively close to that of the Gaussian distribution (Kurt $= 3$). However, their small systematic variation indicates a platykurtic distribution of measured points (flatter than the Gaussian) for the damaged system, while the healthy system shows a leptokurtic density (more peaky distribution). Note that the Gaussian process can be associated with the presence of random external force and/or torque disturbances. The change in kurtosis indicates the additional correlated effect of internal forces in the gear system. The large increase can detect intermittency [21].

To make further progress with the recurrence analysis the corresponding time series have been normalized properly to their standard deviations.

4 The RQA results and discussion

This section reports the results of RQA for time series describing magnitudes of gears system acceleration with damaged and healthy transmission gears. In the search for differences between the considered systems we performed the RQA analysis for 10 consecutive rotation intervals. For each period, recurrence quantifiers defined in the previous section with the assumed critical distance (threshold value) $\varepsilon = 0.5$ and minimal length of a diagonal and vertical line equal to 2 were calculated. Instead of the embedding space estimation [22, 23] we used a 3 dimensional space spanned on the 3 axial acceleration signals (x,y,z).

Using the experimental data, RQA measures were calculated to distinguish between healthy and damaged gears (Figs. 3-13). *RR* values for different revolutions and two sensors are compared in Fig. 3.

As depicted in Fig. 3, *RR* takes similar values. Careful inspection shows that a slightly wider range of *RR* ($RR \in [0.0094, 0.0170]$) and simultaneously the mean value are related to the healthy gears (see $RR \in [0.0104, 0.0126]$ for the damaged gears). Consequently, our main conclusion based on Fig. 3 is that the recurrences occur at the similar level, but their distribution can be different.

The examples of the recurrence plots for one chosen rotation interval (No. 8) are given in Fig. 4. Note that, *RR* is the same here (see Fig. 3a) for sensor No. 1 and fairly similar for sensor No. 2 (see Fig. 3b). The vertical scales are different in Fig. 3a and b. This coincidence (Fig. 3a) makes plausible the comparison of the statistics of the diagonal and vertical lines for both gear systems, i.e. healthy and damaged. Namely, the same *RR* implies the same number of recurrence points

for different dynamical responses reflected in different patterns in Fig. 4. The *RR* matrix for the damaged gear signal looks more reddish because of the resolution (with the same number of recurrence points).

Interestingly, the transition from a healthy to a damaged system is associated with different vertical line structures. The apparent evolution from a more like checkerboard and larger square patterns (Fig. 4b) into a collection of vertical and horizontal short lines (Fig. 4a) resembles the intermittency transition discussed by Klimaszewska and Żebrowski [24]. The larger difference of TT in the two examined cases (healthy and damaged) should also reflect the effect.

Fig. 5 shows the selected RQA parameters (*RR*, DET, *LAM*, $LENTR$, $VENTR$, and TT) versus the threshold value ε for case No. 8 of the same healthy and damaged gear signals obtained from sensor No. 1 (see Fig. 3a). There are visible corresponding lines splitting in the region of small ε for DET, *LAM*, and $VENTR$. Simultaneously, *RR* lines are very close (Fig. 5a). TT lines (Fig. 5f) are also split but for fairly larger ε, while $LENTR$ lines (Fig. 5d) are fairly close in the whole region, making a noticeable difference in order of altitudes $LENTR(\text{healty}) > LENTR(\text{damaged}) \rightarrow LENTR(\text{damaged}) < LENTR(\text{healty})$ for a large enough ε ($\varepsilon \approx 4.1$).

The corresponding recurence plots for RQA parameters along the full time history consisting of 10 rotation intervals. can be found in the next figures (Figs. 6–12). The threshold value ε was fixed as in Fig. 3 ($\varepsilon = 0.5$). Note that the equal *RR* values determine equal number of recurrence points for healthy and damaged gears and make the RQA measures possible to compare.

DET versus consecutive revolution is shown in Fig. 6. Obviously, the DET parameter corresponds to the predictability of the process. It is higher for both H1 and H2 but a more significant change can be noted for D1 and H1 (H1 almost twice higher than D1). Another indicator, corresponds to regularity of the process is i.e. *LMAX* (Fig. 7).

Thus, *LMAX* varies for the healthy gears (H1 and H2) whereas it is flatter for the damaged ones (D1 and D2) but it takes twice higher values, especially for data recorded by the first sensor. On the other hand, those values are quite small as compared to the length of the whole data (6196 points). That might indicate the influence of noise or non periodic behaviour.

Mean length of the diagonal line is shown in Fig. 8. Comparison of the *L* values shows differences for the healthy gear for D1 and H1 (Fig. 8a - sensor No.1). Clearly, indicators calculated for the second sensor (Fig. 8b - sensor No. 2) are different (D2 and H2). Those lengths are quite small, which is typical for non periodic or/and intermittent dynamics [19, 25].

Clear distinction of signals for each sensors can be also found in the values of entropy of the diagonal lines (Fig. 9). Interestingly, the results are different again for sensor No. 1 and 2 like the results of *L* in Fig. 9.

The above inconsistency needs to be clarified. The expected decrease of *L* and even more evidently $LENTR$ in the damaged systems is related to the ordering effect of the increasing nonlinearity (as noted for the sensor No. 1 – Figs. 8a, 9a). However, this explanation is only valid in the limit of small ε which is not reached. This means that, in our system $\varepsilon = 0.5$ is not small. Furthermore *RR*, is fluctuating more in sensor No. 2, which can also cause difficulty estimating other parameters.

More clues about the stability of the power transmission dynamical process can be found in the values of indicators based on statistics of the vertical lines (Figs. 10–12). For instance, Fig. 10 specifies the vertical line distribution. The appearance of vertical lines (Fig. 4) gives some information about fairly small variations of recurrence intervals whereas isolated points indicate the large changes. By means of *LAM* one can see the clear distinction between healthy and damaged system. Thus, *LAM* for a damaged system is smaller which is again the ordering effect of the defect caused by increased nonlinearity.

The following parameters $VMAX$ (Fig. 11) and TT are also larger for a damaged system. The effect is more visible for sensor No. 1 (Fig. 11a and 12a). Interestingly, for sensor No. 2 (Fig. 11b and 12b) the tendency is opposite, in particular for rotation interval No. 7 as the percentage of recurrence of healthy system was smaller for the damaged gear system. This implies the role of *RR* parameter variation which is more significant for sensor No. 2.

Finally, $VENTR$ versus consecutive rotation intervals, plotted in Fig. 13, behaves in a similar way (as compared to that of $VMAX$ and TT – Figs. 11 and 12) with the higher values for the healthy system. The same is for rotation interval No. 7 (for sensor No. 2 – Fig. 12b could be related to disturbances in *RR* (Fig. 3b).

To exclude various fluctuations, we calculated the averages of all examined QRA parameters (for 10 rotation intervals) which are given in Tab. 2.

There is a clear difference between $\overline{DET}$, $\overline{LMAX}$, $\overline{LAM}$, and $\overline{VMAX}$ which confirms the previous particular revolution analysis. This means that, the averaging canceled some interval-to-interval fluctuations.

Our results show clearly that the RQA statistics can be used to distinguish between a healthy system of gears and a damaged gear system. The analysis of results should begin from the estimation of *RR* which is an important parameter and should be used to normalize the results obtained and consequently to compare different time series by the proper choice of ε (in our case ε was selected better for sensor No. 1 than sensor No. 2). Afterwards, any other RQA parameters can be estimated. Most significant differences can be found in the values of DET and *LAM* which were always higher for healthy gears.

In fact the common procedure in an experimental data analysis is based on frequency domain. Comparing a hight frequency limit one can see power spectrum (Fig. 14) for time series of sensor No. 1 and the rotation interval No. 8 in all 3 directions (x, y, and z).

Based on power spectra for *y* and *z* direction one can see peaks with higher amplitude and frequency for damaged gear can be noted. The corresponding values of peaks are much higher than the shaft speed (103 Hz).

That indicates harmonics at high frequency in the damaged but not healthy gear system. Obviously, one can see there is a frequency shift for higher frequencies of the damaged system response appearing in all directions (Figs 14a–c). Simultaneously, power spectra for the gear vibrations are within a narrower range in the presence of defects. This effect is the most transparent in *z* direction (Fig. 14c). The shift of the peaks and the corresponding frequency band shrinking are the effects which accompany defects. In the recurrence approach we can notice the ordering of oscillations which slightly change from interval to interval.

5 Summary and conclusions

In summary, we have applied the nonlinear recurrence based method analysis to experimental data taken from the aviation power transmission. Analysis of experimental data is difficult, mainly due to influence of additional noise that can distort the results [26]. To distinguish a healthy gear transmission from a damaged one, the recurrence indicators are used. Applying the RQA allows for detecting systematic differences in the values of DET and LAM, assumed as quantifiers. Interestingly, the effect is also noted in Kurtosis (Tab. 1). We have also noticed that results may slightly vary with changes of the parameters values (L, $LMAX$, $LENTR$, TT, $VMAX$, $VENTR$) due to a sensor selected. Such a choice implies more implies more careful fixing the value of ε in order to minimize the variations of RR. The averaging procedure applied to the RQA parameters over 10 rotation intervals has helped to cancel their fluctuations (Tab. 2).

Additionally, the examined data indicate stationary vibrations as there are no jumps in recurrences ratios or statistical indicators.

To conclude, the new method of monitoring a gear system is recommended for an industrial environment. The advantage of the recurrence approach is that only two parameters RR and DET identifying a defect instead of observing the whole frequency spectrum of the Fourier analysis in each interval. However, more systematic experiments with different threshold values ε, as well as various kinds of gear defects should be done before the implementation of this method to the industry.

Acknowledgement

The research leading to these results has received partial funding from the European Union Seventh Framework Programme (FP7/2007-2013), FP7 - REGPOT - 2009 - 1, under grant agreement No: 245479.

References

[1] Harris, S.L. 1958. Dynamic loads on the teeth of spur gears. *Proc. Inst. Mech. Eng.* **172**, 87–112.

[2] Parker, R.G., Vijayakar, S.M., Imajo, T. 2000. Nonlinear dynamical response of a spur gear pair: modelling and experimental comparisons. *J. Sound Vib.* **237**, 435–455.

[3] Warmiński, J., Litak, G., Szabelski, K. 2000. Dynamic phenomena in gear boxes. In: *Applied Nonlinear Dynamics and Chaos of Mechanical Systems with Discontinuities* (Wiercigroch, M. & De Kraker, B. editors), Series on nonlinear science A, vol. 28, (World Scientific, Singapore) pp. 177-205.

[4] Guo, Y., Parker, R.G. 2010, Sensitivity of general compound planetary gear natural frequencies and vibration modes to model parameters. *J. Vib. Acoust.* **132**, 011006.

[5] Cooley, C.G., Parker, R.G., Vijayakar S.V. 2011. A frequency domain finite element approach for three-dimensional gear dynamics. *J. Vib. Acoust.* **133**, 041004.

[6] Kahraman, A., Singh, R. 1991. Interactions between time-varying mesh stiffness and clearance nonlinearity in a gear system. *J. Sound Vibr.* **146**, 135–156.

[7] Byrtus, M., Zeman, V. 2011. On modeling and vibration of gear drives influenced by nonlinear couplings. *Mechanism and Machine Theory* **46**, 375–397.

[8] Łazarz, B., Wojnar, G. Madej, H., Czech, P. 2009. Evaluation of gear power losses from experimental test data and analytical methods. *Mechanika* **6**, 56–63.

[9] Lin, J., Parker, R.G. 2002. Parametric instability of planetary gears under mesh stiffness variation. *J. Sound Vibr.* **29**, 411–429.

[10] Litak, G., Friswell, M.I. 2005. Dynamics of a gear system with faults in meshing stiffness. *Nonlinear Dynamics* **41**, 415–421.

[11] Jedliński, Ł., Kisiel, J., Jonak, J. 2009. Diagnosing the condition of gear transmission on the basis of periodic and residual components of the signal spectrum. *Diagnostyka* **49**, 51–67.

[12] Lyons R. G. Understanding Digital Signal Processing, Prentice Hall, New Jersey 2004.

[13] Litak, G., Sawicki, J.T., Kasperek, R. 2009. Cracked rotor detection by recurrence plots. *Nondestructive Testing and Evaluation* **24**, 347–351.

[14] Litak, G., Syta, A., Gajewski, J., Jonak, J. 2010. Detecting and identifying nonstationary courses in the ripping head power consumption by recurrence plots. *Meccanica* **45**, 603–608.
[15] Nichols, J.M., Trickey, S.T., Seaver, M. 2006. Damage detection using multivariate recurrence quantification analysis. *Mech. Syst. Signal Process.* **20**, 421–437.
[16] Eckmann, J.-P., S.O. Kamphorst, S.O., Ruelle, D. 1987. Recurrence plots of dynamical systems. *Europhys. Lett.* **5**, 973–977.
[17] Webber Jr. C.L., Zbilut, J.P. 1994. Dynamical assessment of physiological systems and states using recurrence plot strategies. *J. App. Physiol.* **76**, 965–973.
[18] Marwan, N. 2003. 'Encounters with Neighbours: Current Development of Concepts Based on Recurrence Plots and their Applications. PhD Thesis, Universität Potsdam, Potsdam.
[19] Marwan, N., Romano, M.C., Thiel, M., Kurths, J. 2007. Recurrence plots for the analysis of complex systems. *Physics Reports* **438**, 237–329.
[20] Marwan, N., Commandline recurrence plots, http:// www.agnld.uni- potsdam.de/ ∼marwan/ 6.download/ rp.php (May 10th 2009).
[21] Sen, A.K., Litak, G., Edwards, K.D., Finney, C.E.A., Daw, C.S., Wagner R.M. 2011. Cyclic heat release variability with transition from spark ignition to HCCI in internal combustion engines, *Applied Energy* **88**, 1557–1567.
[22] Takens, F. 1981. *Detecting Strange Attractors in Turbulence*, Lecture Notes in Mathematics, Vol. 898 (Springer, Heidelberg) pp. 366–381.
[23] Kantz, H., Schreiber, T. 1997. *Non-linear Time Series Analysis*, (Cambridge University Press, Cambridge).
[24] Klimaszewska, K., Żebrowski, J.J. 2009. Detection of the type of intermittency using characteristic patterns in recurrence plots. *Phys. Rev.* E **80**, 026214.
[25] Litak, G., Wiercigroch, M., Horton, B.W, Xu, X. 2010. Transient chaotic behaviour versus periodic motion of a parametric pendulum by recurrence plots. *Z. Angew. Math. Mech.* 90, 33–41.
[26] Mo, E., Naess, A. 2009. Nonsmooth dynamics by path integration: an example of stochastic and chaotic response of a meshing gear pair. *J. Comput. Nonlinear Dynam.* **4**, 034501.

Table 1. Statistic properties of time series. The signal D1 stands for acceleration of the faulty gear recorded by the first sensor, H1 - acceleration of the healthy gear; the signals D2 and H2 - obtained from the second sensor.

Signal	$\bar{x}$ [m/s^2]	$\bar{y}$ [m/s^2]	$\bar{z}$ [m/s^2]	σ_x [m/s^2]	σ_y [m/s^2]	σ_z [m/s^2]	$Kurt_x$	$Kurt_y$	$Kurt_z$
D1	0.119	0.458	0.547	108.25	107.30	99.82	2.929	2.575	2.879
H1	0.111	0.139	0.198	113.54	201.88	210.91	3.109	3.061	3.164
D2	0.557	0.153	0.157	138.17	127.17	108.36	3.032	2.954	2.913
H2	0.217	0.192	0.464	197.66	161.55	214.48	3.214	3.195	3.162

Table 2. Average values of RQA for all presented revolutions Nos. 1-10 with $\varepsilon = 0.5$. The signal D1 stands for acceleration of the faulty gear recorded by the first sensor, H1 - acceleration of the healthy gear; the signals D2 and H2 - obtained from the second sensor.

Signal	$\overline{RR}$	$\overline{DET}$	$\overline{LMAX}$	$\overline{L}$	$\overline{LENTR}$	$\overline{LAM}$	$\overline{VMAX}$	$\overline{TT}$	$\overline{VENTR}$
D1	0.029	0.345	22.4	2.4	0.853	0.528	10.9	2.4	0.859
H1	0.032	0.571	44.9	2.6	1.076	0.742	17.0	2.8	1.280
D2	0.033	0.371	28.0	2.5	0.958	0.553	13.9	2.5	0.984
H2	0.035	0.482	39.4	2.5	0.929	0.675	16.7	2.6	1.133

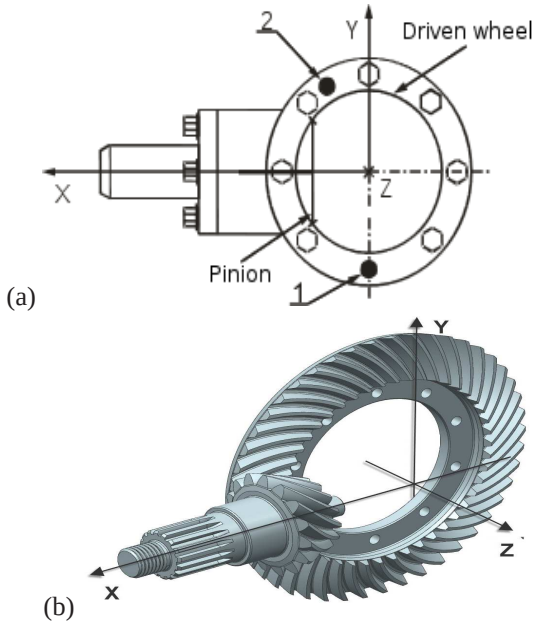

Fig. 1. (a) Location of the sensors on the shaft where 1 and 2 stand for first and second sensor, respectively [11]. (b) 3D schematic view of a gear system.

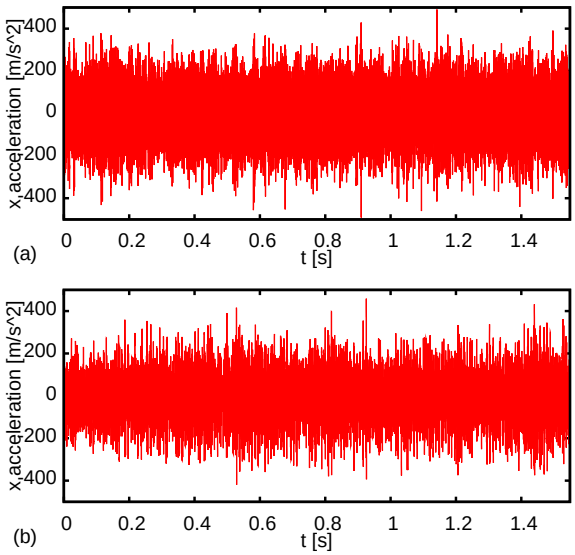

Fig. 2. Acceleration time series describing acceleration in x direction of system with a pair of damaged (1D - (a)) and healthy (1H - (b)) gears, obtained by the sensor No. 1

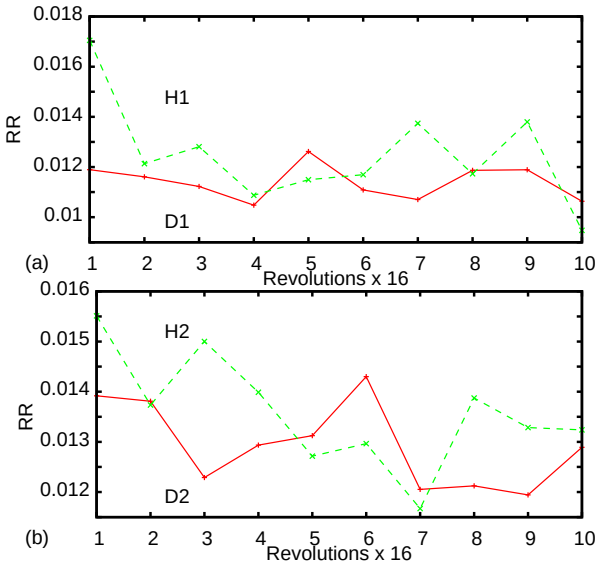

Fig. 3. (color online) Recurrence rate RR for healthy; H1 (a), H2 (b) (green dashed lines) and damaged; D1 (a), D2 (b) (red full lines) gears calculated with $\varepsilon = 0.5$.

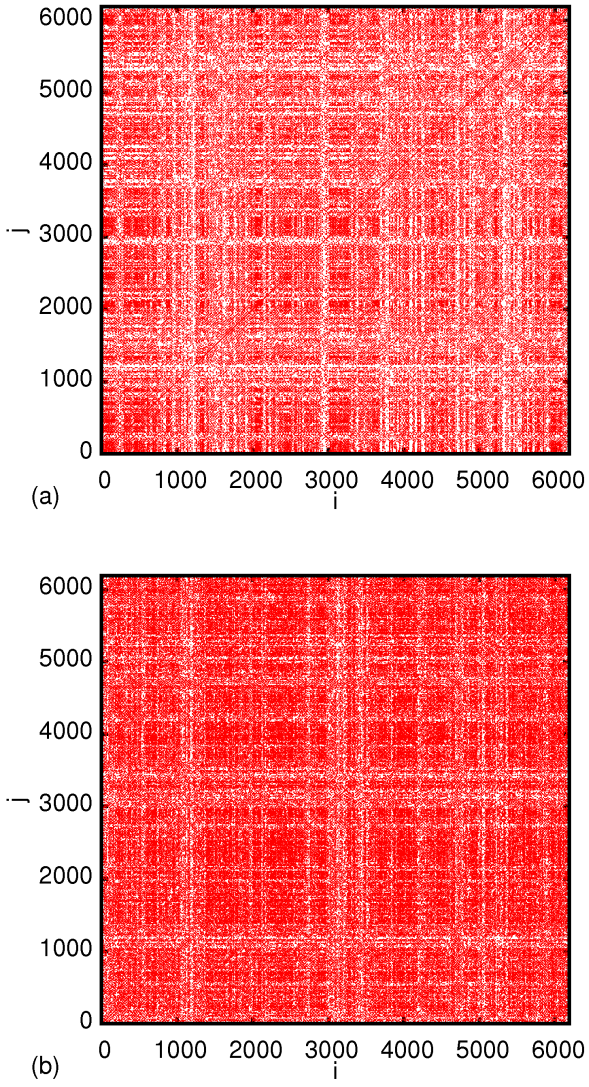

Fig. 4. Recurrence plots (with $\varepsilon = 0.5$) for the rotation interval No. 8 for the signals obtained from the sensor No. 1 (see Fig. 3a), and different gear systems: healthy (a) and damaged (b) ones, respectively. The embedding space consist of x, y, and z acceleration components.

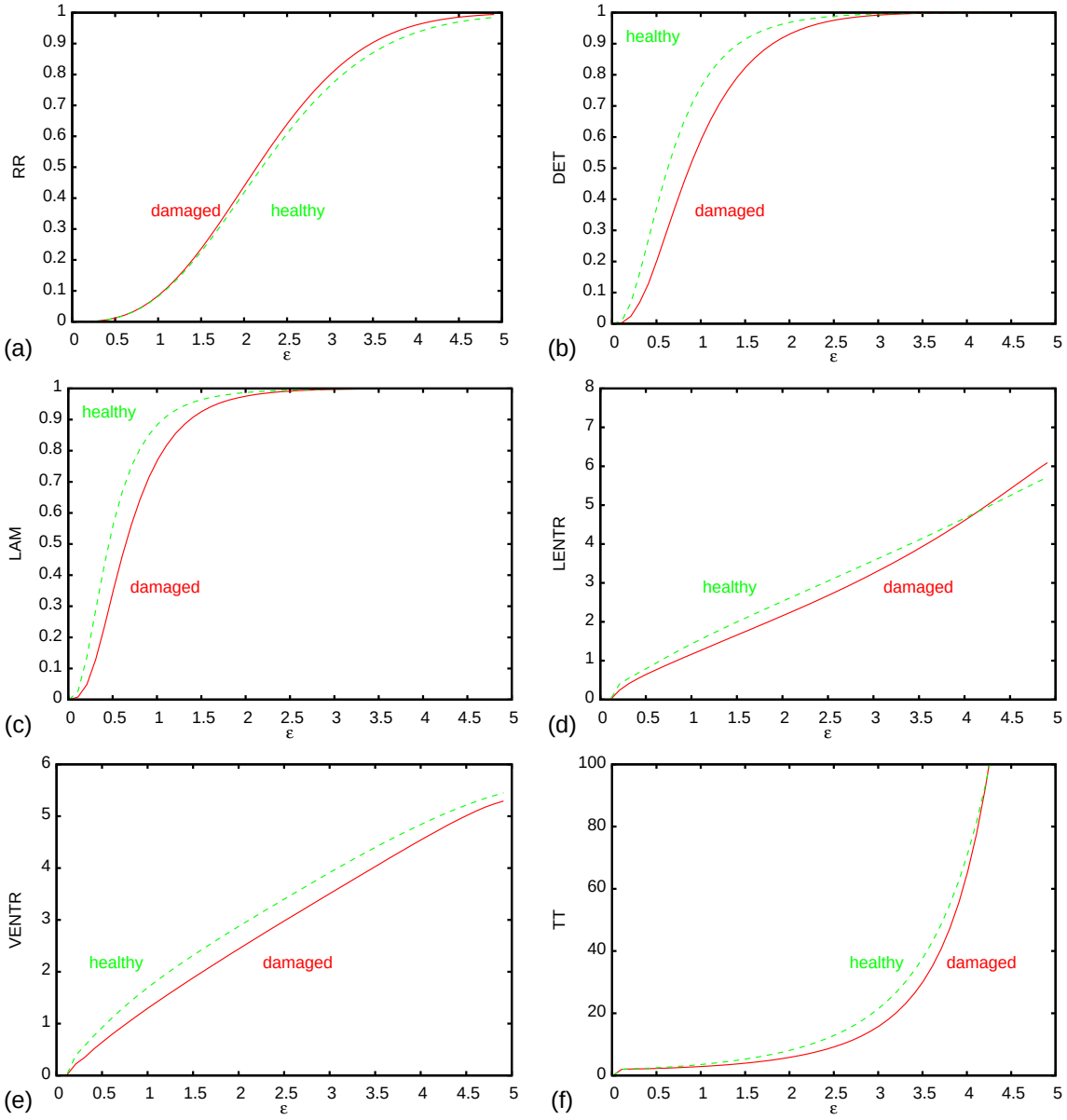

Fig. 5. (color online) Selected RQA parameters versus ε for the case No. 8 of the signals obtained from the sensor No. 1 (see Fig. 3a), and different gear systems: healthy (green dashed lines) and damaged (red full lines), respectively. The embedding space consists of x, y, and z acceleration components.

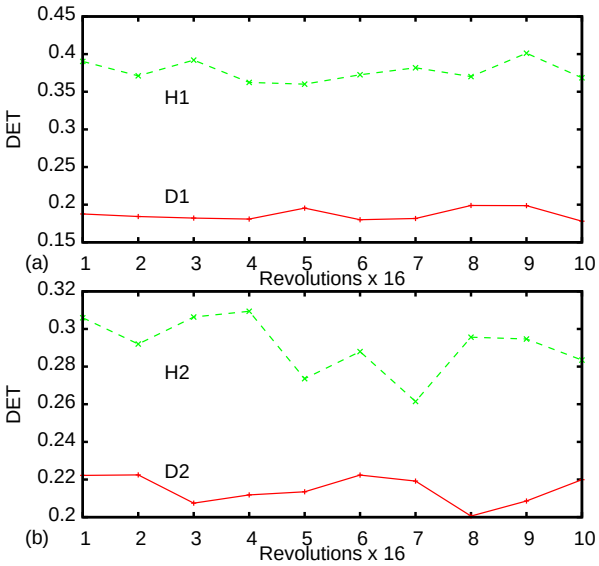

Fig. 6. (color online) Determinism DET for healthy; H1 (a), H2 (b) (green dashed lines) and damaged; D1 (a), D2 (b) (red full lines) gears calculated with $\varepsilon = 0.5$.

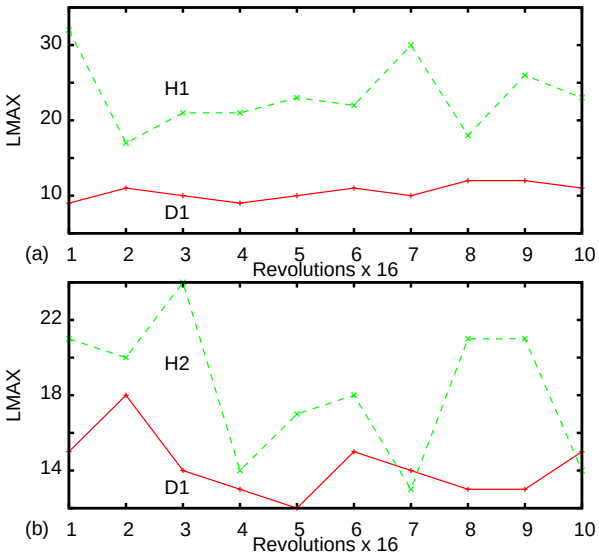

Fig. 7. (color online) $LMAX$ for healthy; H1 (a), H2 (b) (green dashed lines) and damaged; D1 (a), D2 (b) (red full lines) gears calculated with $\varepsilon = 0.5$.

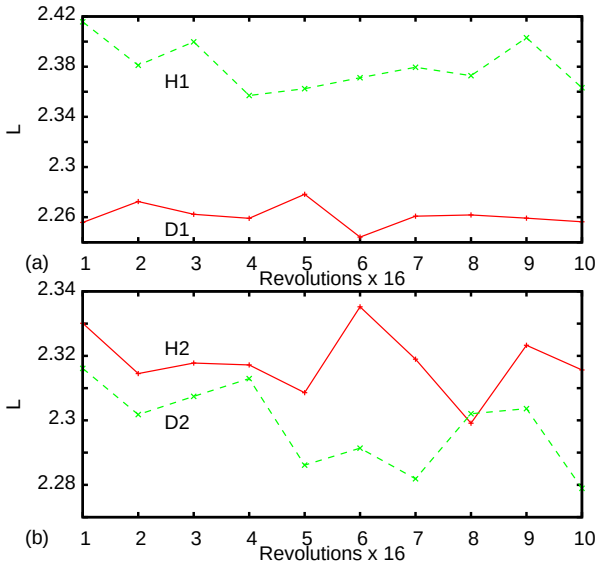

Fig. 8. (color online) L for healthy; H1 (a), H2 (b) (green dashed lines) and damaged; D1 (a), D2 (b) (red full lines) gears calculated with $\varepsilon = 0.5$.

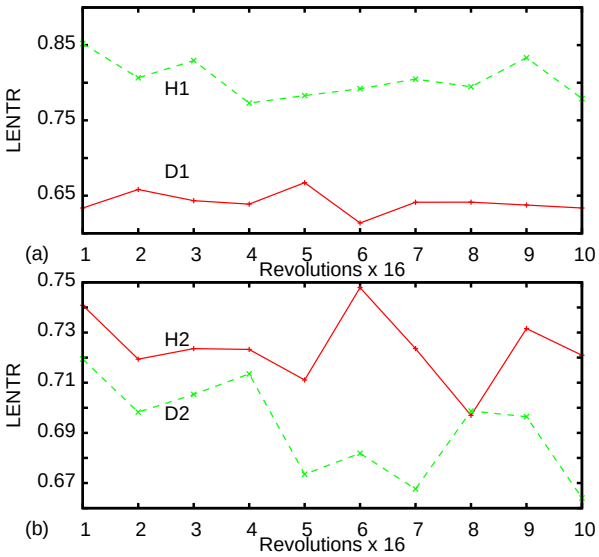

Fig. 9. (color online) $LENTR$ for healthy; H1 (a), H2 (b) (green dashed lines) and damaged; D1 (a), D2 (b) (red full lines) gears calculated with $\varepsilon = 0.5$.

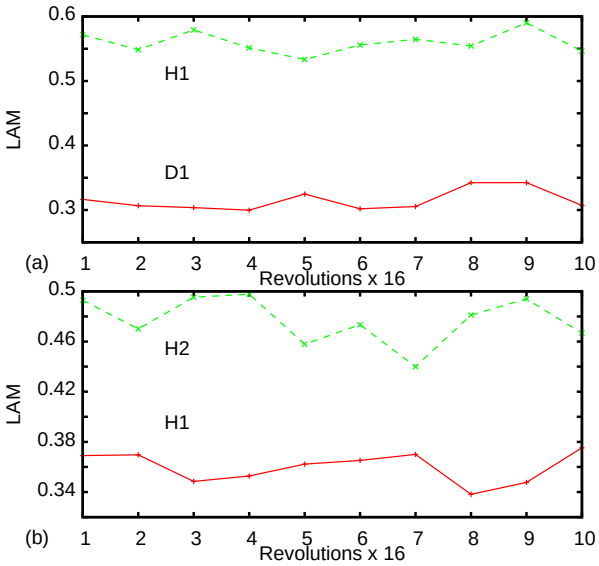

Fig. 10. (color online) Laminarity LAM for healthy; H1 (a), H2 (b) (green dashed lines) and damaged; D1 (a), D2 (b) (red full lines) gears calculated with $\varepsilon = 0.5$.

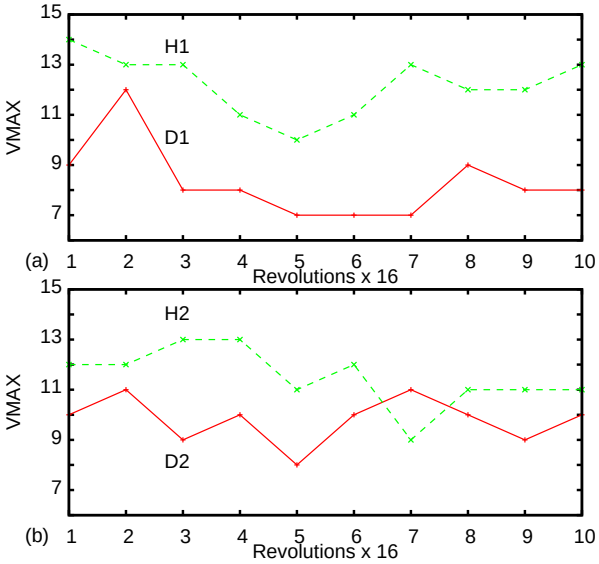

Fig. 11. (color online) $VMAX$ for healthy; H1 (a), H2 (b) (green dashed lines) and damaged; D1 (a), D2 (b) (red full lines) gears calculated with $\varepsilon = 0.5$.

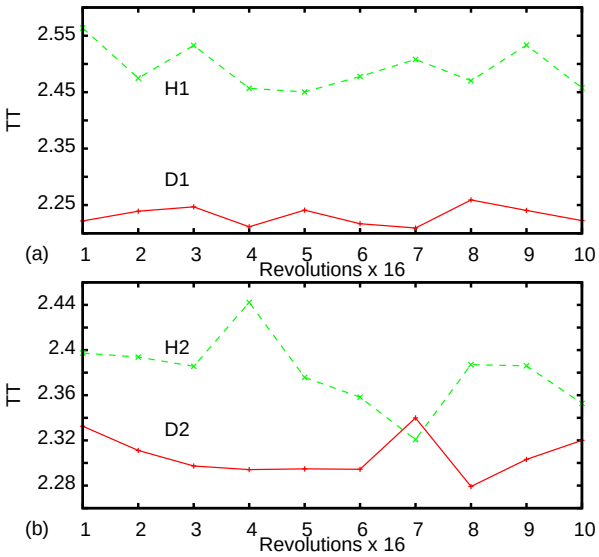

Fig. 12. (color online) Trapping time TT for healthy; H1 (a), H2 (b) (green dashed lines) and damaged; D1 (a), D2 (b) (red full lines) gears calculated with $\varepsilon = 0.5$.

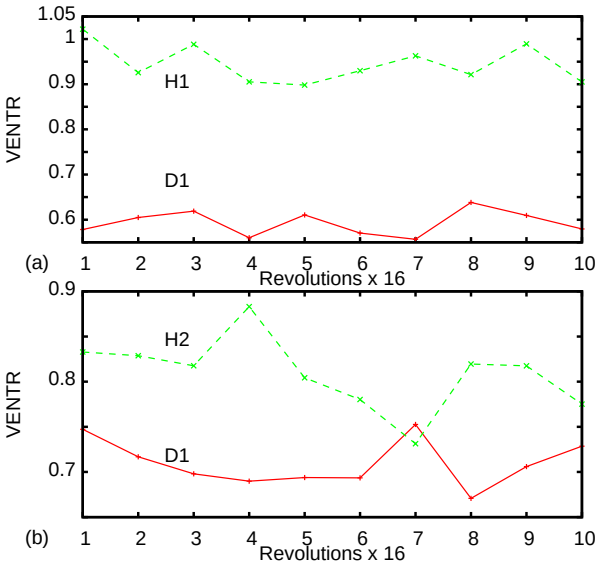

Fig. 13. (color online) $VENTR$ for healthy; H1 (a), H2 (b) (green dashed lines) and damaged; D1 (a), D2 (b) (red full lines) gears calculated with $\varepsilon = 0.5$.

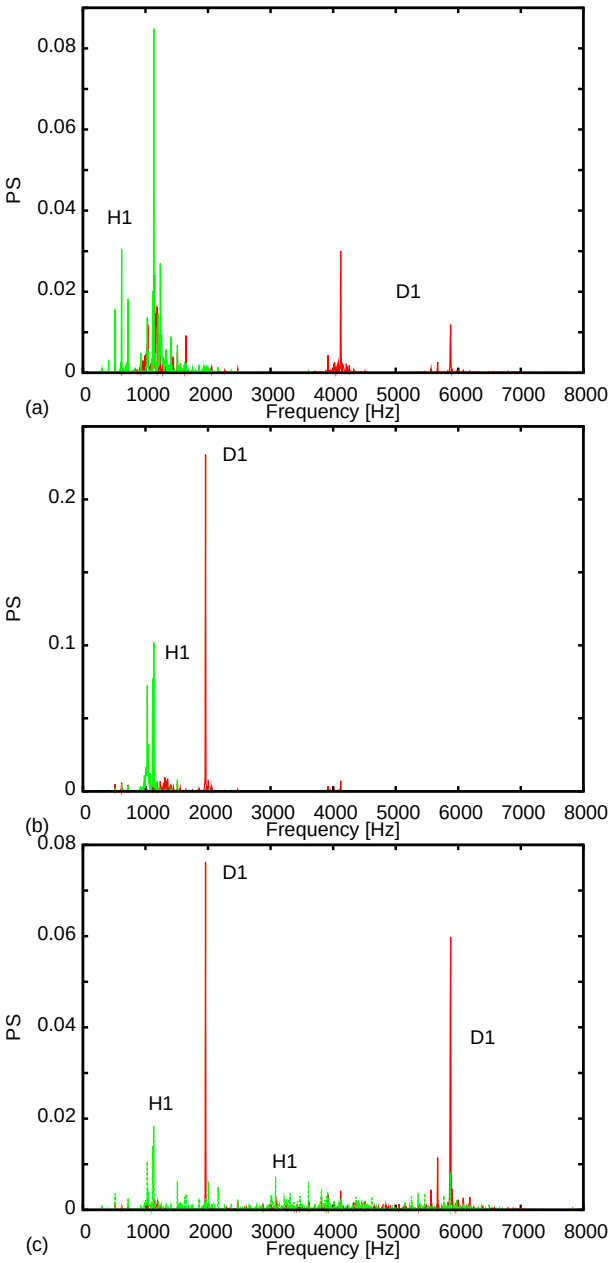

Fig. 14. (color online) Power spectra for the revolution No. 8 estimated for x acceleration (a), y acceleration (b), z acceleration (c) for the healthy (green) and damaged (red) transmission gears. Note that the damaged system spectra have more localized and larger frequencies.